Electronic properties of multiwalled carbon nanotubes in an embedded vertical array

Jun Li,[a),b)] Ramsey Stevens,[b)] Lance Delzeit, Hou Tee Ng,[c)] Alan Cassell,[b)] Jie Han,[b)] and M. Meyyappan

NASA Ames Research Center, Moffett Field, California 94035

We demonstrate integration of carbon nanotubes into large scale vertically aligned electrode arrays, by filling the as-grown samples with conformal SiO_2 using chemical vapor deposition. Subsequent mechanical polishing yields a flat surface with only the very ends of the nanotube array exposed. The electronic properties of individual carbon nanotubes in the array are measured using current-sensing atomic force microscopy. These vertical nanotube arrays are suitable for fabricating various electronic devices and sensors. © *2002 American Institute of Physics.*
[DOI: 10.1063/1.1496494]

Carbon nanotubes (CNTs) have attracted attention in the fabrication of transistors,[1–3] memories,[4] logic gates,[5–7] and chemical sensors.[8] The fabrication of these devices typically rely on CNTs randomly laid or grown on flat substrates. For applications such as field-emission displays and electrodes, vertically aligned CNTs with controlled density are desired.[9] Recently, ultrahigh density of nanotransistors were reported using vertically aligned CNT arrays.[10] We report here an approach to build vertically aligned CNT arrays which involves gap filling of the as-grown CNT array with SiO_2 using chemical vapor deposition (CVD) followed by mechanical polishing. These steps, common in semiconductor processing, produce a mechanically strong array with only the tips exposed. The uniform length and good alignment of CNTs in the embedded array have advantages in field emission devices, vertical transistors, and nanoelectrode based chemical sensors.[11,12] We also report here the topography and conductivity distribution at the surface of the electrode using current-sensing atomic force microscopy (CSAFM) and the electronic properties of individual CNTs using $I–V$ spectroscopy at various spots on the electrode.

First, vertically aligned multiwalled carbon nanotubes (MWCNTs) were grown on silicon using an inductively coupled plasma (ICP) as reported previously.[13] For comparison, we obtained MWCNT samples (Nanolab Inc., MA) grown by dc hot-filament plasma CVD.[14] The average height of the MWCNTs is 3–10 μm. The ICP samples have a thin (10 nm) Al layer at the bottom while the hot filament sample has a thicker (~200 nm) Ti or Mo layer. The MWCNT arrays were subjected to a gap filling with SiO_2 at 700°–750° in a CVD furnace using tetraethylorthosilicate (TEOS) vapor at 300 mTorr.[15] The SiO_2 film was thick enough to bury all CNTs. The top surface of the samples after TEOS CVD was found completely electrically insulated from the underlying metal film and CNTs. A mechanical polishing step was then followed to remove the excess SiO_2 until electrical conductivity between two spots on the surface can be measured. The

polishing procedure produced a rather flat surface with uniform CNT length of about 3 μm buried in SiO_2 matrix.

Figure 1 shows the scanning electron microscope (SEM) images of the initial MWCNT array, the sample after TEOS CVD and mechanical polishing, respectively. Very good alignment can be observed both at 45° and normal to the surface. After TEOS CVD, the sample was cleaved in the middle [Fig. 1(c)]. The TEOS CVD produces a quite conformal SiO_2 film covering both the underlying metal layer and each CNT. The film around the top part of the CNTs is slightly thicker than that at the bottom due to better accessibility for TEOS vapor. The high density of the MWNT array results in the SiO_2 film at the top part merged into grains over several microns in size while some irregular voids (20–500 nm) remain at the bottom. Even though the voids penetrate deep in the film, they do not reach the metal underlayers. Electrochemical measurements with such samples in solution indicated that normally the metal films are not accessible to electrolytes. The voids can be reduced by adopting a slower deposition rate at lower TEOS partial pressure or by reducing the CNT density. The SiO_2 filling greatly
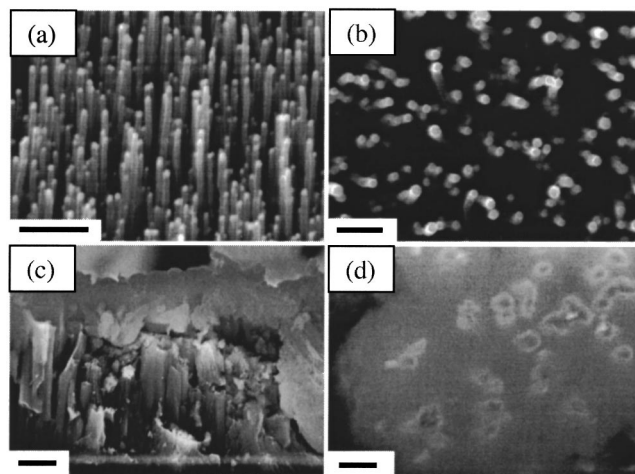

FIG. 1. SEM images of the initial MWCNT array from dc hot-filament CVD (a) 45° view, and (b) top view, (c) cross section image of the array after TEOS CVD, (d) top view after mechanical polishing. The scale bars are 1 μm, 500 nm, 2 μm, and 500 nm, respectively.

[a)]Electronic mail: jli@mail.arc.nasa.gov
[b)]Also at: ELORET Corporation.
[c)]Also at: SETI Institute.

improves the mechanical strength of the CNT array and allows it to sustain the aggressive mechanical polishing. The mechanical polishing removed the SiO_2 on the top surface as well as part of the CNTs, producing a composite film with individual CNTs embedded in the SiO_2 matrix. CNTs were found to preserve their integrity and alignment during these steps. The top view SEM image in Fig. 1(d) clearly shows a similar distribution of CNT ends as the original sample.

Previous works on CNT transport mostly studied a sidewall contact geometry by laying down CNT on a surface.[1–7] The embedded CNT array here provides a model system in which the electronic properties can be studied by point contact at the tube ends. This system provides different information from other studies. Particularly, in previous MWCNT devices, mainly the outmost shell is in good contact with electrodes and dominates their electronic properties.[16,17] It is of interest to investigate the electronic properties of the embedded vertically aligned CNTs in which many graphitic shells are in contact with the metal contact. Since the polished sample presents a rather flat surface, AFM techniques can be readily employed and additional electronic properties can be measured with a Pt-coated tip connected with a current sensing module[18] (Molecular Imaging, AZ). Figure 2(a) shows the deflection image of the polished sample. Most CNTs uniformly protrude out of the SiO_2 surface by about 2 nm, which is likely due to their high mechanical resilience.[19] CNTs exhibit a uniform diameter around 100 nm which agrees well with the initial sample in Fig. 1(a). Figure 2(b) shows the current-sensing image obtained simultaneously with the deflection image by applying a dc bias between the metal underlayer and the Pt-coated AFM tip. SiO_2 is highly insulating, so current can be observed only when the AFM tip is in contact with CNTs. The size of the conducting spots correlates very well with the physical size of CNTs in Figs. 1(a) and 2(a). We switched the bias from $+8.0$ to -12.0 mV in the middle of the image frame scanning topdown. As a result, the polarity of the current flipped over with the bias as shown in Fig. 2(c). Interestingly, the density and the amplitude of the conducting spots increase when the magnitude of the bias is increased, indicating the sensitive $I–V$ correlation.

Most studies on electronic properties of CNTs rely on measuring the $I–V$ curve of individual CNTs or CNT bundles one at a time after they have been laid or grown horizontally on the surface and connected with metal electrodes.[1–7] With the CSAFM and embedded CNT arrays, $I–V$ curves of hundreds of individual CNTs can be investigated quickly. Figure 3(a) shows a typical $I–V$ curve for an embedded MWCNT array prepared using hot-filament CVD. These CNTs are highly conductive. The $I–V$ curve is essentially a straight line within the instrumental limits (± 10 nA). The resistance of this single MWCNT is about 310 kΩ. Since the CSAFM can apply only a small bias (± 3 mV) before the detector saturates, we also used a four-probe station (Desert Cryogenics, AZ) linked with a semi-conductor parameter analyzer (6045B, Agilent, CA). As shown in the inset of Fig. 3(a), a perfect linear curve is observed within ± 5.0 V giving a resistance of 5.2 kΩ, likely corresponding to about 60 MWCNTs in parallel contact with the 25 μm diam probe. In comparison, if the AFM tip locates
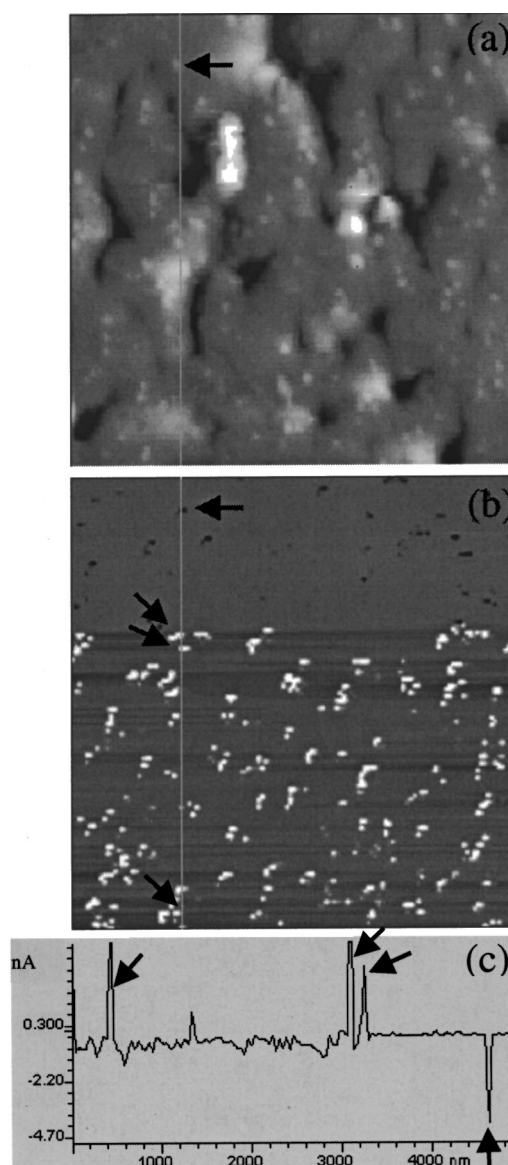

FIG. 2. (a) The deflection and (b) the current-sensing image of an embedded MWCNT array after the polishing step simultaneously obtained with a current-sensing AFM. The scan range is 5×5 μm^2. The voltage between the substrate and the tip is changed from $+8.0$ to -12.0 mV in the middle of the image frame scanning topdown. (c) The current profile along the vertical lines indicated in (a) and (b). The spikes correspond to the higher conductivity of carbon nanotubes [indicated by the arrows in (a) and (b)] compared to the insulating SiO_2 matrix.

any spot of SiO_2 surface, the $I–V$ curve shows a flat line at 7 ± 1 pA (due to the instrument offset), indicating a very good electrical insulation. $I–V$ measurements on an embedded MWCNT array prepared by ICP CVD with CSAFM are shown in Fig. 3(b). These CNTs showed similar alignment but a bigger variation in tube diameter (30–80 nm) compared to the hot-filament CVD sample. As a result, the $I–V$ curve shows a big variation, but most data fall in between the two curves presented. These $I–V$ curves show a gap varying from 0.3 to 1.0 V. A small portion (much less than one third) of the CNTs was found to exhibit linear $I–V$ curves. The $I–V$ measured on a four-probe station show a nonlinear feature even though the probe is in contact with tens of CNTs. Note that these samples have only a thin layer of metal and any observed gap may be due to the contribution from both underlying metal film and CNTs. Raman scattering analysis
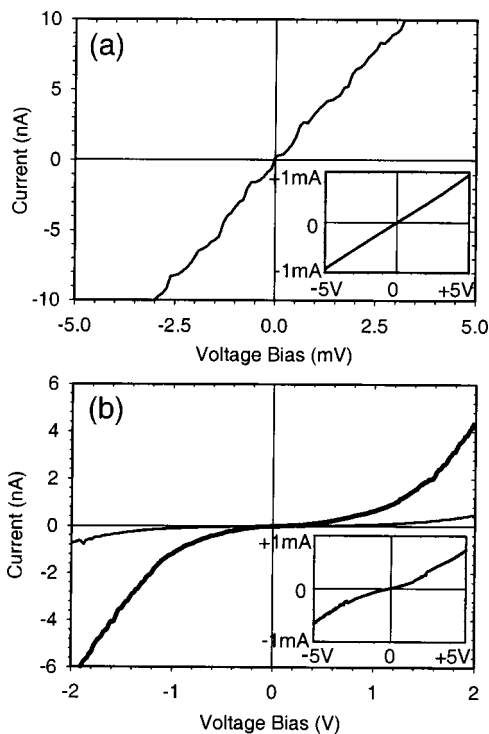
FIG. 3. $I-V$ curves of individual MWCNTs in the embedded array obtained with current-sensing AFM. The insets show four-probe station data corresponding to multiple parallel MWCNTs. (a) Nanotubes from dc hot-filament CVD and (b) nanotubes from inductively coupled plasma CVD.

the other end. This will produce a high resistance as well as defect-sensitive electronic properties.

In summary, we report fabrication of embedded vertically aligned carbon nanotube arrays and characterization of electronic properties of individual MWCNTs using CSAFM. Our approach is useful to fabricate large-scale nanoelectronic devices in a vertical geometry such as crossbar-addressed transistor network, field emitters, and nanoelectrode arrays.

of the two samples do not distinguish them as metallic versus semiconducting but do show differences in relative ratio between different bands indicating that ICP samples are more defective.

The resistance of the metallic MWCNTs here (about 300 kΩ) is much higher than previous reports using the sidewall contact geometry (<30 kΩ)[20,21] even though our tube diameter is much bigger. This is likely due to the fact that we have only point contact with the tube ends. A recent theoretical study[22] shows that the contact length (area) between metal and CNTs is critical for the conductance which drops dramatically if the contact length is less than 10 nm. In addition, the plasma CVD samples do not have perfect semi-infinite cylindrical graphitic layer structure as those produced by laser ablation;[20,21] instead, they are highly defective carbon fiber-like structures with graphitic layers nonparallel to the tube axis.[13,14] Electrons are expected to cross over graphitic layers in the process transporting from one end of the tube to

[1] S. J. Tans, A. R. M. Verschueren, and C. Dekker, Nature (London) **393**, 49 (1998).

[2] M. S. Fuhrer, J. Nygard, L. Shih, M. Forero, Y.-G. Yoon, M. S. C. Mazzoni, H. J. Choi, J. Ihm, S. G. Louie, A. Zettl, and P. L. McEuen, Science **288**, 494 (2000).

[3] C. W. Zhou, J. Kong, E. Yenilmez, and H. Dai, Science **290**, 1552 (2000).

[4] T. Rueckes, K. Kim, E. Joselevich, G. Y. Tseng, C. L. Cheung, and C. M. Lieber, Science **289**, 94 (2000).

[5] V. Derycke, R. Martel, J. Appenzeller, and Ph. Avouris, Nano Lett. **1**, 453 (2001).

[6] A. Bachtold, P. Hadley, T. Nakanishi, and C. Dekker, Science **294**, 1317 (2001).

[7] X. L. Liu, C. Lee, C. W. Zhou, and J. Han, Appl. Phys. Lett. **79**, 3329 (2001).

[8] J. Kong, N. R. Franklin, C. W. Zhou, M. G. Chapline, S. Peng, K. Cho, and H. Dai, Science **287**, 622 (2000).

[9] L. Nilsson, O. Groening, C. Emmenegger, O. Kuettel, E. Schaller, L. Schlapbach, H. Kind, J.-M. Bonard, and K. Kern, Appl. Phys. Lett. **76**, 2071 (2000).

[10] W. B. Choi, J. U. Chu, K. S. Jeong, E. J. Bae, J.-W. Lee, J.-J. Kim, and J.-O. Lee, Appl. Phys. Lett. **79**, 3696 (2001).

[11] V. P. Menon and C. R. Martin, Anal. Chem. **67**, 1920 (1995).

[12] J. K. Campbell, L. Sun, and R. M. Crooks, J. Am. Chem. Soc. **121**, 3779 (1999).

[13] L. Delzeit, I. McAninch, B. A. Cruden, D. Hash, B. Chen, J. Han, and M. Meyyappan, J. Appl. Phys. **91**, 6027 (2002).

[14] Z. P. Huang, J. W. Xu, Z. F. Ren, J. H. Wang, M. P. Siegal, and P. N. Provencio, Appl. Phys. Lett. **73**, 3845 (1998).

[15] S. M. Sze, *VLSI Technology* (McGraw-Hill, New York, 1988), pp. 249–260.

[16] S. Frank, P. Poncharal, Z. L. Wang, and W. A. De Heer, Science **280**, 1744 (1998).

[17] P. G. Collins, M. S. Arnold, and P. Avouris, Science **292**, 706 (2001).

[18] G. Leatherman, E. N. Durantini, D. Gust, T. A. Moore, A. L. Moore, S. Stone, Z. Zhou, P. Rez, Y. Z. Liu, and S. M. Lindsay, J. Phys. Chem. B **103**, 4006 (1999).

[19] H. Dai, J. H. Hafner, A. G. Rinzler, D. T. Colbert, and R. E. Smalley, Nature (London) **384**, 147 (1996).

[20] R. Martel, T. Schmidt, H. R. Shea, T. Hertel, and Ph. Avouris, Appl. Phys. Lett. **73**, 2447 (1998).

[21] P. J. de Pablo, E. Graugnard, B. Walsh, R. P. Andres, S. Datta, and R. Reifenberger, Appl. Phys. Lett. **74**, 323 (1999).

[22] N. Mingo and J. Han, Phys. Rev. B **64**, 201401 (2001).